symmetry

IMPACT FACTOR 2.2

CITESCORE 5.4

Review

Extraordinary Nature of the Nucleon Scalar Charge and Its Densities as a Signal of Nontrivial Vacuum Structure of QCD

Masashi Wakamatsu

Special Issue

Chiral Symmetry, and Restoration in Nuclear Dense Matter

Edited by

Prof. Dr. Kazuo Tsushima, Prof. Dr. Anthony Thomas and Prof. Dr. Myung Ki Cheoun

MDPI

https://doi.org/10.3390/sym16111481

symmetry

MDPI

Review

Extraordinary Nature of the Nucleon Scalar Charge and Its Densities as a Signal of Nontrivial Vacuum Structure of QCD

Masashi Wakamatsu

KEK Theory Center, Institute of Particle and Nuclear Studies, High Energy Accelerator Research Organization (KEK), Oho 1-1, Tsukuba 305-0801, Ibaraki, Japan; wakamatu@post.kek.jp

Abstract: It is widely known that the nucleon scalar charge is proportional to the pion–nucleon sigma term as one of the important low-energy observables of QCD. Especially interesting to us is the physics of the nucleon scalar charge densities. This comes from the fact that the corresponding operator has the same quantum number as the physical vacuum. It indicates unusual behavior of the nucleon scalar density as a function of the distance r from the nucleon center. Namely, it would not be reduced down to zero at the spatial infinity but rather approach some nonzero constant corresponding to the vacuum quark condensate. Naturally, this unique nature of the nucleon scalar density in the position space also affects the corresponding density in the momentum space, i.e., the corresponding parton distribution function (PDF) as a function of the Bjorken variable x. This PDF is known as the chiral-odd twist-3 PDF $e(x)$. We argue that $e(x)$ is likely to have a delta-function-type singularity at $x = 0$ and that the appearance of this singularity can be interpreted as a signal of the nontrivial vacuum structure of QCD.

Keywords: nucleon scalar charge density; nontrivial vacuum structure of QCD; chiral-odd twist-3 PDF $e(x)$; existence of delta-function singularity at $x = 0$; pion–nucleon sigma-term sum rule

check for updates

Citation: Wakamatsu, M. Extraordinary Nature of the Nucleon Scalar Charge and Its Densities as a Signal of Nontrivial Vacuum Structure of QCD. *Symmetry* **2024**, *16*, 1481. https://doi.org/10.3390/sym16111481

Academic Editor: Sergei Odintsov

Received: 2 October 2024
Revised: 25 October 2024
Accepted: 4 November 2024
Published: 6 November 2024

1. Introduction

It is well known that the nucleon scalar charge is related to the pion–nucleon sigma term, which is one of the important low-energy observables [1,2]. However, since the standard model of elementary particles is a V-A (vector and axial-vector) theory, there is no external electro-weak current, which directly couples to the nucleon scalar charge as well as to the tensor charge [3,4]. In recent years, these quantities have attraced wide interest in the search of physics beyond the standard model, which also allows S–T (scalar and tensor) couplings [5,6]. In the present paper, we demonstrate that far more interesting than the nucleon scalar charge itself is its densities in the coordinate space as well as in the momentum space. Why are they interesting? The ultimate reason can be traced back to the fact that the corresponding operator has the same quantum number as the physical vacuum of QCD. As is widely known, as a consequence of spontaneous chiral-symmetry breaking (χSB), the QCD vacuum is believed to be characterized by nonzero quark condensate, i.e., nonzero scalar quark density. This implies that the nucleon scalar density as a function of the distance r from the nucleon center is expected to show the following abnormal behavior. Namely, as the distance r increases, the nucleon scalar density does not attenuate to zero, but it would rather approach nonzero values corresponding to the vacuum quark condensate. A natural question is whether this unique nature of the nucleon scalar charge density would show up somewhere in physical observables. The purpose of the present concise review is to show that we can answer the above question affirmatively.

2. Physics Behind the Nucleon Scalar Charge

There already exist several lattice QCD calculations of the pion–nucleon sigma term $\Sigma_{\pi N}$ or the nucleon scalar charge $\bar{\sigma}$ [7–9]. They are related as $\Sigma_{\pi N} = m_{ud}\,\bar{\sigma}$, where m_{ud} is

the average mass of the up and down quarks. To obtain a rough idea about the magnitude of $\bar{\sigma}$ or $\Sigma_{\pi N}$, here, we quote the results of the recent lattice QCD simulation by Alexandrou et al. [9]. (Note that the scalar coupling g_S in their notation is identified with the nucleon scalar charge $\bar{\sigma}$ in our notation.) Their prediction for $\bar{\sigma}$ is given as a sum of four terms:

$$\bar{\sigma} \;=\; \bar{\sigma}(u+d(conn)) \;+\; \bar{\sigma}(u+d(disc)) \;+\; \bar{\sigma}(s) \;+\; \bar{\sigma}(c), \tag{1}$$

with

$$\bar{\sigma}(u+d\,(conn)) \;=\; 20.4(1.6), \quad \bar{\sigma}(u+d\,(disc)) \;=\; 3.04(59), \tag{2}$$

$$\bar{\sigma}(s) \;=\; 1.00(13), \quad \bar{\sigma}(c) \;=\; 0.175(36). \tag{3}$$

Here, $\bar{\sigma}(u+d\,(conn))$ and $\bar{\sigma}(u+d\,(disc))$, respectively, stand for the contribution of the connected and disconnected diagrams coming from the up and down quarks, while $\bar{\sigma}(s)$ and $\bar{\sigma}(c)$ represent the contributions from the strange and charm quarks. One sees that the contribution of the connected diagrams dominates over that of the disconnected diagrams. However, it should be kept in mind that the separation into the connected and disconnected pieces in the lattice QCD simulation does not necessarily correspond to directly observable separation. The final prediction for the pion–nucleon sigma term is also given as [9]

$$\Sigma_{\pi N} \;=\; m_{ud}\,\bar{\sigma} \;\simeq\; 41.6\,(3.8)\,\mathrm{MeV}, \tag{4}$$

although the value of m_{ud} is not explicitly written in their paper. Anyhow, this value seems roughly consistent with the empirical one obtained from the analysis of the low-energy pion–nucleon scattering data [10–12].

To understand the fundamental importance of the pion–nucleon sigma term, it would be useful to briefly recall the physics behind the nucleon scalar charge. First, let us remember the theoretical prediction of the MIT bag model as a prototype low-energy effective theory of the nucleon [13]. Its prediction is given as follows:

$$\bar{\sigma} \;=\; \langle N\,|\int \bar{\psi}(\boldsymbol{r})\,\psi(\boldsymbol{r})\,d^3r\,|N\rangle \;=\; N_c\int_0^\infty \Big\{f(r)^2 \;-\; g(r)^2\Big\}\,r^2\,dr. \tag{5}$$

Here, $N_c = 3$ is the number of colors, while $f(r)$ and $g(r)$ are the upper and lower components of the radial wave function in the MIT bag model. Since the radial wave functions are normalized as

$$\int_0^\infty \Big\{f(r)^2 \;+\; g(r)^2\Big\}\,r^2\,dr \;=\; 1, \tag{6}$$

and since the upper component $f(r)$ dominates over the lower component $g(r)$, we are inevitably led to an inequality,

$$\int_0^\infty \Big\{f(r)^2 \;-\; g(r)^2\Big\}\,r^2\,dr \;<\; 1. \tag{7}$$

This in turn leads to the remarkable inequality

$$\bar{\sigma} \;<\; N_c \;=\; 3. \tag{8}$$

For reasonable choice of the quark mass m_{ud}, this gives a too small $\Sigma_{\pi N}$, which is largely incompatible with the existing empirical information for the pion–nucleon sigma term [10–12]. We must therefore conclude that the naive quark model with only three valence quark degrees of freedom sizably underestimates the magnitude of $\Sigma_{\pi N}$.

A fatal shortcoming of the naive three-quark models in the scalar channel is also clear from its prediction for the nucleon scalar charge density in the coordinate space. A typical prediction of the naive three-quark models of the nucleon for the scalar density is

illustrated in Figure 1. (The scalar quark density $\rho_S(r)$ shown in Figure 1 is normalized as $4\pi \int_0^\infty \rho_S(r)\, r^2\, dr = \bar{\sigma}$, with $\bar{\sigma}$ being the nucleon scalar charge. Since the unit of r is given by fm (fermi or femtometre), the unit of $\rho_S(r)$ here is fm^{-3}.) As one sees, the scalar density takes a maximum value at the center of the nucleon, and it smoothly attenuates to zero as the distance r from the nucleon center becomes large and approaches infinity. One should recognize that this contradicts our expectation that, at least in the region far apart from the nucleon center, the scalar quark density must coincide with the nonzero value of the vacuum quark condensate as long as we believe the scenario that the spontaneous breaking on the chiral symmetry generates nonzero vacuum quark condensate [14]. As we shall see in the next section, the chiral quark soliton model (CQSM) is a very unique effective model of the nucleon, which can simultaneously reproduce the nontrivial vacuum quark condensate and the local structure of the nucleon scalar charge density.

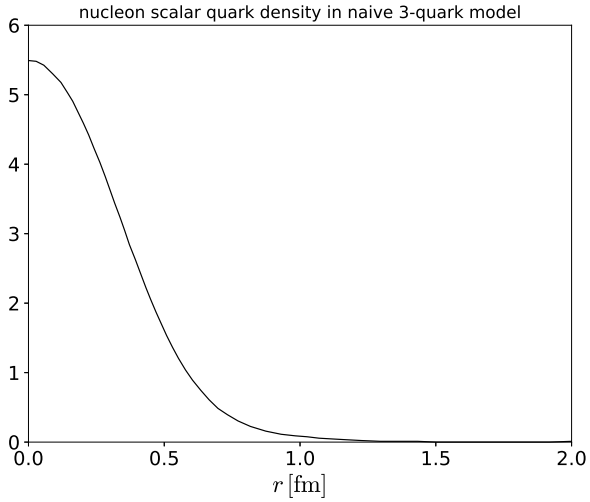

Figure 1. Typical prediction of the naive three-quark model for the nucleon scalar charge density $\rho_S(r)$ in the coordinate space.

3. Brief Introduction to the Chiral Quark Soliton Model

The chiral quark soliton model (CQSM) is a low-energy effective model of baryons first introduced by Diakonov et al. based on the instanton-liquid picture of the QCD vacuum [15]. The effective Lagrangian of the CQSM is given by

$$\mathcal{L}_{CQSM} \;=\; \bar{\psi}(x)\left(i\gamma^\mu \partial_\mu \;-\; M\, e^{\,i\gamma_5 \boldsymbol{\tau}\cdot\boldsymbol{\pi}(x)/f_\pi}\right)\psi(x), \tag{9}$$

where $\psi(x)$ and $\boldsymbol{\pi}(x)$ represent the effective quark and pion fields, while M stands for the effective quark mass (or the constituent quark mass) of the order of 400 MeV. Note that there is no kinetic term for the pion in this lagrangian, which implies that the pion field in this model is not an independent field but rather a dependent field of quarks (or the quark–anti-quark composite). The effective pion action $S_{eff}[\boldsymbol{\pi}]$ obtained from this lagrangian can be defined by formally carrying out the path integration over the quark field,

$$Z \;=\; \int \mathcal{D}\boldsymbol{\pi} \int \mathcal{D}\psi\, \mathcal{D}\psi^\dagger\; e^{\,i\int d^4x\, \mathcal{L}_{CQSM}} \;=\; \int \mathcal{D}\boldsymbol{\pi}\; e^{\,i\, S_{eff}[\boldsymbol{\pi}]}. \tag{10}$$

It is known that if we use the derivative-expansion-type approximation in the three-flavor case, we obtain an effective meson action of the following structure,

$$\begin{aligned} S_{eff}[\boldsymbol{\pi}] \;&=\; \text{Skyrmion action with Wess-Zumino term} \\ &+\; \text{destabilizing 4-th derivative term} \\ &+\; \cdots . \end{aligned} \tag{11}$$

Unfortunately, different from the original Skyrmion action, the existence of the destabilizing 4th derivative term does not allow for the existence of a stable soliton-like solution. The basic idea of the CQSM is to construct a stable soliton-like localized solution *without* relying upon derivative-expansion-type approximation. Basically, it is a relativistic mean-field theory for quark fields. We start with the assumption that the pion field, which plays the role of the mean field for quarks, takes the hedgehog form as follows similar to the famous Skyrme model,

$$\boldsymbol{\pi}(\boldsymbol{r}) \;=\; \hat{\boldsymbol{r}}\, F(r), \tag{12}$$

where the function $F(r)$ is supposed to satisfy the following boundary condition,

$$F(0) \;-\; F(\infty) \;=\; n\,\pi \tag{13}$$

with $n\,(=1)$ being the so-called winding number of the effective pion field. Under the presence of this mean field, the quark field obeys the following Dirac equation,

$$H\,|m\rangle \;=\; E_m\,|m\rangle, \tag{14}$$

with

$$H \;=\; \frac{\boldsymbol{\alpha}\cdot\nabla}{i} \;+\; M\,\beta\,(\cos F(r) \;+\; i\,\gamma_5\,\sin F(r)). \tag{15}$$

A characteristic feature of this Dirac equation with the topologically twisted hedgehog mean field is that one deep single-quark bound state appears from the positive energy continuum of the above Dirac Hamiltonian. (See Figure 2 for illustration.) We call this particular single-quark level the *valence quark orbital*.

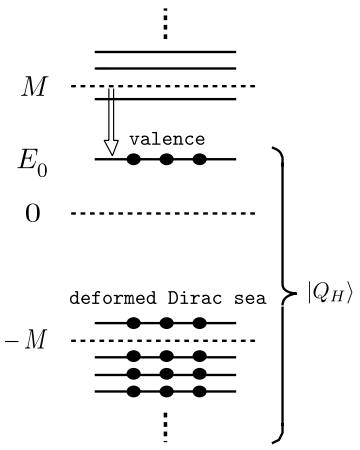

Figure 2. Characteristic behavior of the single-quark energy levels under the mean field of hedgehog shape.

An object having baryon number one with respect to the physical vacuum is obtained by putting $N_c\,(=3)$ quarks into this valence orbital as well as all the negative energy (Dirac-sea) orbitals. This baryon number one object with respect to the physical vacuum is sometimes called the quark hedgehog denoted as $|Q_H\rangle$. Accordingly, the total energy of this quark hedgehog is given as a sum of the valence quark contribution and the vacuum polarization contribution as

$$E_{static} \;=\; N_c\,E_0 \;+\; E_{v.p.}, \tag{16}$$

where E_0 is the single-particle energy of the valence quark level, while the vacuum polarization contribution represents the Casimir energy resulting from the polarization (deformation) of the Dirac-sea quark orbitals and given by

$$E_{v.p.} \;=\; N_c \left(\sum_{m\,(E_m<0)} E_m \;-\; \sum_{k\,(\epsilon_k<0)} \epsilon_k \right). \tag{17}$$

That is, the Casimir energy is given as a sum of all the energies of quarks in the negative-energy Dirac-sea orbitals. Here in Equation (17), the 2nd term represents the subtraction of the Dirac-sea energy of the physical vacuum. (The physical vacuum of the model is obtained by letting $F(r) \to 0$.) The most probable pion field configuration is then determined on the basis of the stationary requirement for the total energy $E_{static}[F(r)]$,

$$\frac{\delta}{\delta F(r)} E_{static}[F(r)] \;=\; 0. \tag{18}$$

This requirement combined with the above Dirac equation is reduced to a self-consistent Hartree problem which can be solved by the numerical method of Kahana and Ripka [16]. (See [17] for more detail about the actual calculation method.) After self-consistency is fulfilled, the hedgehog pion field, which was originally introduced as an external mean field for quarks, becomes an implicit functional of the quark fields.

Actually, the vacuum polarization energy given by Equation (17) contains ultraviolet (logarithmic) divergence. Often, this ultraviolet divergence is removed with the use of the Pauli–Villars regularization, which means the following replacement of the effective action

$$S_{eff}[\boldsymbol{\pi}] \;\to\; S^{M}_{eff}[\boldsymbol{\pi}] \;-\; \left(\frac{M}{M_{PV}}\right)^2 S^{M_{PV}}_{eff}[\boldsymbol{\pi}], \tag{19}$$

where M_{PV} is a Pauli–Villars cutoff mass. However, since the vacuum quark condensate contains *quadratic divergence*, the single subtraction is not enough and we need double-term Pauli–Villars subtraction as used in [18],

$$S_{eff}[\boldsymbol{\pi}] \;\to\; S^{M}_{eff}[\boldsymbol{\pi}] \;-\; \sum_{i=1}^{2} c_i\, S^{\Lambda_i}_{eff}[\boldsymbol{\pi}], \tag{20}$$

The four subtraction parameters c_1, c_2, Λ_1, and Λ_2 are determined so as to remove the quadratic and logarithmic divergence of the effective action and to reproduce the empirical value of vacuum condensate and the correct pion kinetic energy term in the effective pion action [18]. Once these parameters are fixed, the model is known to reproduce low-energy observables of the nucleon as well as the various quark distributions of the nucleon remarkably well [19–25].

To convince the reliability of the CQSM, we show below its characteristic predictions related to the most important parton distribution functions at the twist-2 level. Probably, one of the remarkable predictions of the CQSM is that it reproduces the observed small quark spin contribution to the total nucleon spin fairly well. We show in Figure 3 the prediction of the CQSM for the longitudinal quark spin $\Delta\Sigma$ and the longitudinal gluon spin Δg in the nucleon as compared with the empirical information. Here, the scale dependencies of $\Delta\Sigma$ and Δg are taken into account by using the evolution (DGLAP) equation at the next-leading order (NLO) under the assumption that $\Delta g = 0$ at the initial energy scale $Q^2_{ini} = 0.30\,\mathrm{GeV}^2$, which we identify as the energy scale of our effective quark model. One sees that the CQSM predicts fairly small quark spin contents in the nucleon, and it is qualitatively consistent with the empirical information. We emphasize that the small prediction of the CQSM for $\Delta\Sigma$ is deeply connected with its nucleon picture as a rotating hedgehog object. The time-dependent rotation of the hedgehog mean field necessarily enhances the contribution of the quark orbital angular momentum, which in turn reduces the contribution of the intrinsic quark spin.

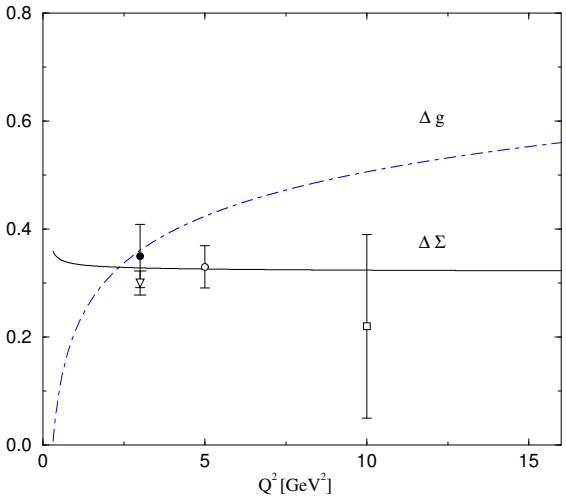

Figure 3. The CQSM prediction of quark spin $\Delta\Sigma$ [26] as compared with the old experimental data from the SMC group [27] and the newer data from the COMPASS [28,29] and HERMES groups [30].

Next, Figure 4 shows the predictions of the CQSM for the longitudinally polarized structure functions of the proton, the neutron and the deuteron as compared with the corresponding experimental data by the SMC group [27], the Compass group [28,29], and the HERMES group [30]. We can say that the agreement with the empirical information is encouraging especially in view of the fact that the predictions of the CQSM are almost parameter free.

Still, another prominent feature of the CQSM is that it can give reliable predictions about the sea-quark distributions or the anti-quark distributions in the nucleon. This greatly owes to its field theoretical nature, which takes account of the deformation (or the vacuum polarization) of the Dirac sea under the presence of the hedgehog mean field in a nonperturbative manner. It is empirically known that the distribution functions of the anti-quarks in the proton is not flavor symmetric; i.e., the distribution of the $\bar{d}$-quark dominates over that of the $\bar{u}$-quark inside the proton. It is widely known that this flavor asymmetry of anti-quark distribution can be explained by the effects of a pion cloud at least qualitatively. The CQSM can explain this feature more qualitatively again without introducing additional free parameters. Figure 5 shows the predictions of the CQSM for the $\bar{d}(x) - \bar{u}(x)$ distribution as well as the ratio $\bar{d}(x) \,/\, \bar{u}(x)$ in comparison with the corresponding experimental data from the Hermes and FNAL-E866/NuSea group as well as the old data from NA51. We can say that the CQSM reproduces the characteristic features of the empirical observations fairly well at least qualitatively.

Very interestingly, the CQSM predicts the flavor asymmetry also for the longitudinally polarized sea-quark (anti-quark) distributions. It turns out that the model predicts that $\Delta\bar{u}(x)$ dominates over $\Delta\bar{d}(x)$. The flavor asymmetry of the longitudinally polarized anti-quark distributions is not yet firmly established with the same accuracy as the flavor asymmetry of the unpolarized anti-quark distributions. Here, in Figure 6, we make a preliminary comparison of the predictions of the CQSM with the empirical DSSV fit [31]. One sees that the qualitative agreement between the theory and the empirical fit is encouraging. Although we cannot show more examples because of the limitation of space, we can say with confidence that the QCSM provides us with a reliable basis to investigate the internal substructure of the nucleon.

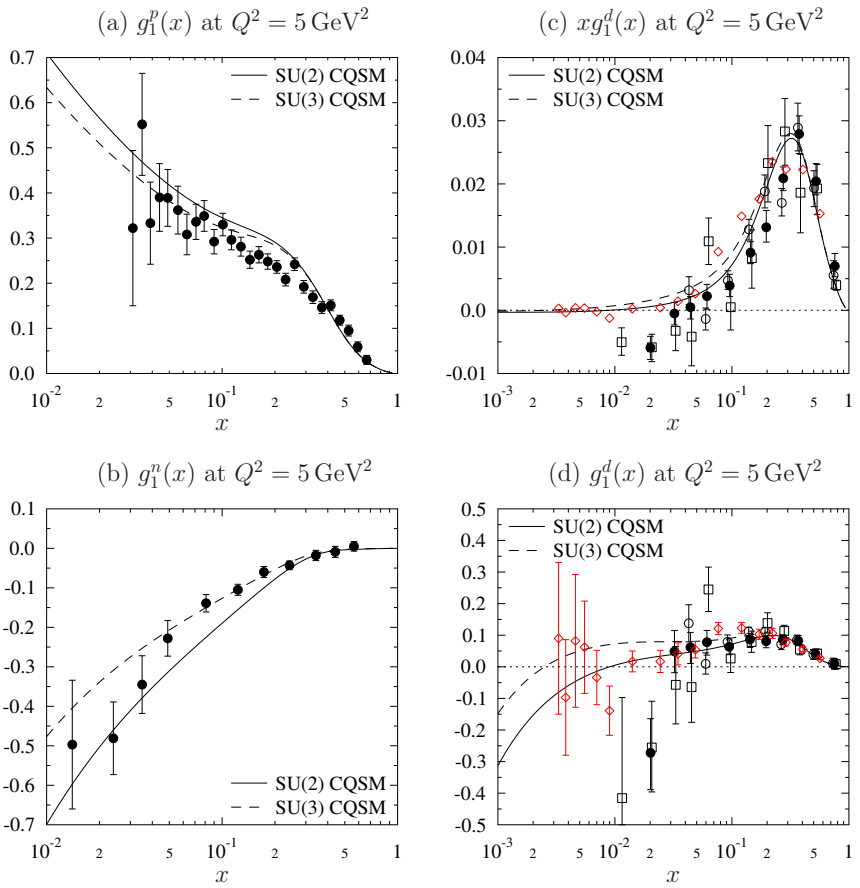

Figure 4. The CQSM predictions for the longitudinally polarized structure functions for the proton, the neutron and the deuteron [26] as compared with the old experimental data from the SMC group [27] and the newer data (red in color) from the COMPASS group [28,29]. For reference, the prediction of the flavor SU(3) version of the CQSM is also shown.

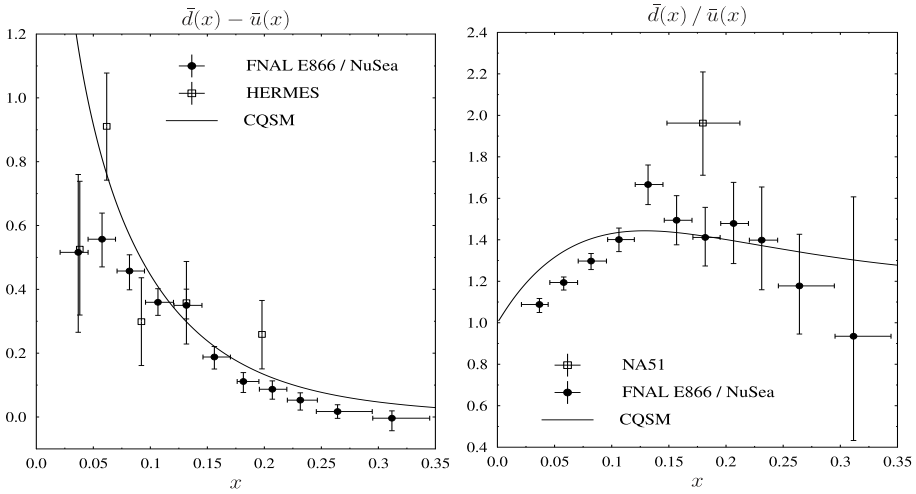

Figure 5. The predictions of the CQSM for the $\bar{d}(x) - \bar{u}(x)$ distribution and the $\bar{d}(x) \,/\, \bar{u}(x)$ [24] in comparison with the corresponding experimental data from the Hermes [32] and FNAL-E866/NuSea groups [33] as well as the old data from NA51 [34].

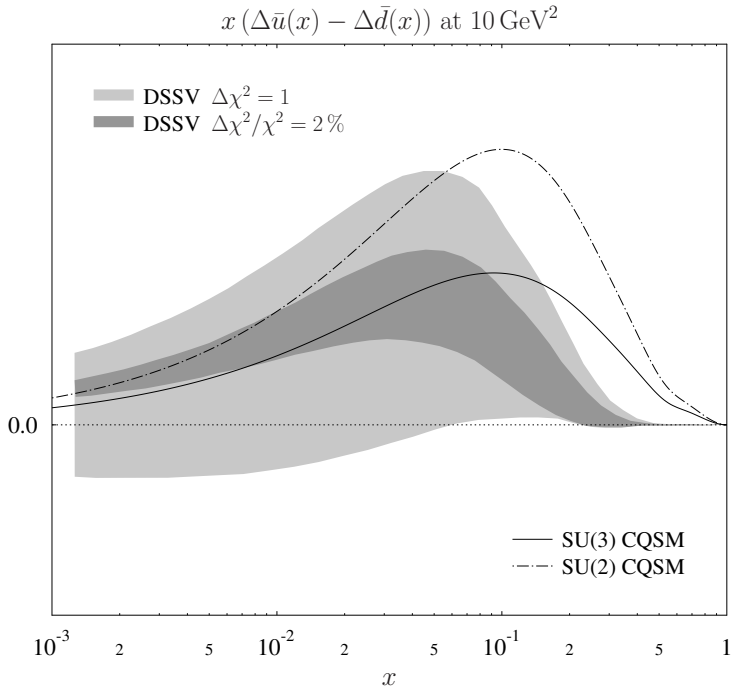

Figure 6. The CQSM predictions for the flavor asymmetry of the longitudinally polarized anti-quark distribution $x\,(\Delta\bar{u}(x) - \Delta\bar{d}(x))$ [24] in comparison with the empirical DSSV fit [31]. For reference, the prediction of the flavor SU(3) version of the CQSM is also shown.

4. Nucleon Scalar Charge Density Predicted by the Chiral Quark Soliton Model

Figure 7 shows the prediction of the CQSM for the nucleon scalar density in the coordinate space [18,35]. (Note that the nucleon scalar charge density in Figure 7 is normalized as $4\pi \int_0^\infty [\rho_S(r) - \rho_S(r=\infty)]\, r^2\, dr = \bar{\sigma}$, with $\bar{\sigma}$ being the nucleon scalar charge.) As one sees, the contribution of the three valence quarks smoothly attenuates to zero as the distance from the nucleon center becomes large, as is the case with the prediction of the naive three-quark model. Remarkably, however, the contribution of the negative energy Dirac-sea quarks does not attenuate to zero, but it approaches a negative nonzero value, which is nothing but the value of the vacuum quark condensate in the QCD vacuum. (We recall that the effective action of the CQSM was constructed so as to reproduce the vacuum quark condensate of the QCD vacuum.) This confirms that the CQSM can explain the vacuum quark condensate and the nontrivial local structure of the nucleon scalar charge density at the same time [18,35]. A question is whether this highly nontrivial behavior of the nucleon scalar density, i.e.,

$$\bar{\sigma}(r) \;\equiv\; \langle N\,|\bar{\psi}(\boldsymbol{r})\,\psi(\boldsymbol{r})\rangle_r \;\overset{r\to\infty}{\to}\; \text{nonzero constant}, \tag{21}$$

appears in some observables?

Note that the Fourier transform of a constant gives a Dirac's delta function. This implies that the nonzero vacuum condensate contained in the nucleon scalar charge density in coordinate space may appear as a delta-function singularity in the scalar charge density (form factor) in momentum space. Unfortunately, the Fourier transform of the local scalar charge density of the nucleon would not correspond to any direct observables. As we shall see below, the relevant quantity here is the nucleon scalar charge density as a function of the momentum variable x of Bjorken or Feynman. It is the chiral-odd twist-3 quark distribution function customarily denoted as $e(x)$.

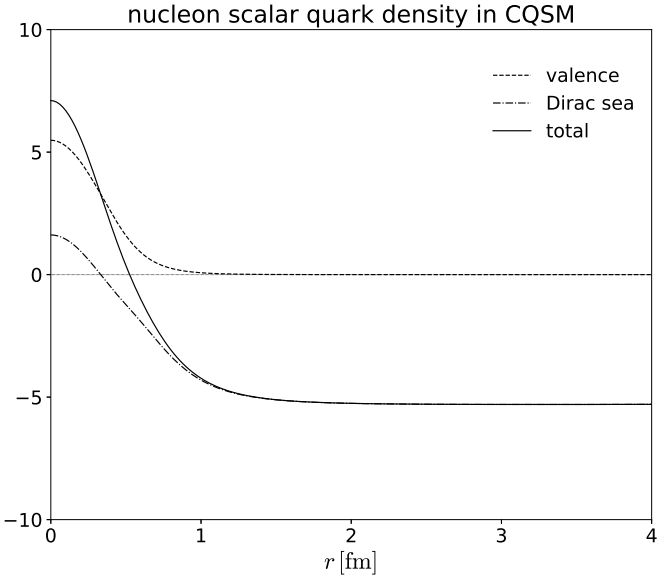

Figure 7. Prediction of the CQSM for the nucleon scalar charge density in the coordinate system. The dashed and dash–dotted curves, respectively, stand for the contribution of the three quarks in the valence level and that of the negative energy Dirac-sea quarks.

5. Twist-3 PDF $e(x)$ as a Nucleon Scalar Density in a Momentum Space

As shown in Table 1, up to the twist-4 order, there are nine independent quark distribution functions (see [36], for example). Hereafter, we call them parton distribution functions or simply PDFs.

Table 1. Nine independent quark distribution functions with twists 2, 3, and 4.

Twist-2	Twist-3	Twist-4
$f_1(x) = q(x)$	$e(x)$	$f_4(x)$
$g_1(x) = \Delta q(x)$	$h_2(x)$	$g_3(x)$
$h_1(x) = \Delta_T q(x)$	$g_T(x)$	$h_3(x)$

For example, $f_1(x)$ or $q(x)$ is the familiar unpolarized PDF of the nucleon, $g_1(x)$ or $\Delta q(x)$ is the longitudinally polarized PDF, and $h_1(x)$ or $\Delta_T q(x)$ is the so-called transversity distribution of the nucleon. Of our particular interest here is $e(x)$, which is classified into a chiral-odd twist-3 PDF. Why is it interesting? The reason is two-fold. First, the 1st moment of $e(x)$ (i.e., its integral over the Bjorken or Feynman variable x) gives the nucleon scalar charge, which is proportional to the pion–nucleon sigma term. Second, the possible existence of Dirac's delta-function-type singularity in $e(x)$ was already suggested by Koike and Burkardt within the framework of perturbative QCD [37] (see also [38]). Unfortunately, the physical origin of this delta-function singularity is not fully understood within the framework of perturbative QCD. However, as we have already suggested, the highly nontrivial structure of the nucleon scalar density predicted by the CQSM might generate a delta-function singularity in the scalar charge density in some momentum space. The correctness of this expectation was shown independently in the paper by Schweitzer [39] and that by ourselves [40]. In these papers, it was shown that the nonperturbative origin of the delta-function singularity in $e(x)$ can be traced back to the infinite-range quark–quark correlation of scalar type in the nucleon and that the existence of this infinite-range correlation is inseparably connected with the nontrivial vacuum structure of QCD, i.e., the spontaneous χSB, and the resulting nonzero vacuum quark condensate. One might wonder why the vacuum property comes into a hadron observable. As already pointed out, it is

related to the previously mentioned extraordinary nature of scalar quark density of the nucleon, which lives in the nontrivial QCD vacuum.

Incidentally, a recent paper [41] by Ma and Zhang attracted renewed interest in the existence or non-existence of the delta-function-type singularity in the twist-3 PDF $e(x)$. According to them, within the framework of perturbative QCD, the delta-function-type singularities certainly exist, but they cancel out among themselves. Soon after, however, their conclusion was criticized in the papers by Bhattacharya et al. [42] and also by Hatta and Zhao [43]. They argued that the treatment by Ma and Zhang is not justified, because it neglects the light-front (LF) zero mode within the framework of the LF quantization, which is vital for describing the nonperturbative vacuum of QCD. In any case, it is clear that the perturbative QCD may be able to predict the existence of the delta-function singularity in $e(x)$, but it has no ability to predict the proportionality constant of this delta-function term. We absolutely need some nonperturbative framework like lattice QCD or some skillfully crafted effective theory of the nucleon which takes account of the nontrivial vacuum structure of our real world.

At this point, it is useful to recall the theoretical definition of the chiral-odd twist-3 PDF $e(x)$ given as

$$e(x) \;=\; M_N \int_{-\infty}^{\infty} \frac{dz_0}{2\,\pi}\; e^{\,-\,i\,x\,M_N\,z_0}\; E(z_0), \tag{22}$$

with

$$E(z_0) \;=\; \langle N \,|\, \bar{\psi}\Big(-\,\frac{z}{2}\Big)\,\psi\Big(\frac{z}{2}\Big)\,|N\rangle\Big|_{z_3=-z_0,\,z_\perp=0}. \tag{23}$$

That is, the PDF $e(x)$ is given as a Fourier transform of the correlation function $E(z_0)$ of the nucleon, which measures the light-cone (LC) quark–quark correlation of scalar type in the physical nucleon. (See Figure 8 for the meaning of the coordinate z.)

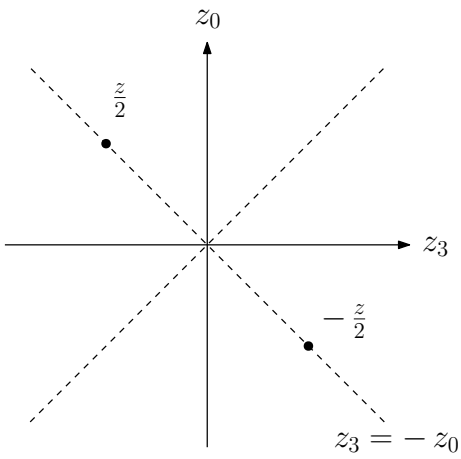

Figure 8. Schematic figure showing the two points separated on the light cone.

The existence of the delta-function singularity in $e(x)$ implies the following behavior of the correlation function $E(z_0)$:

$$E(z_0) \;\overset{z_0\to\infty}{\longrightarrow}\; \text{nonzero constant}, \tag{24}$$

i.e., the existence of an infinite-range LC quark–quark correlation of scalar type. We have already shown that well outside the nucleon, its (local) scalar charge density approaches a nonzero value of vacuum quark condensate. However, what we want to really know here is the asymptotic behavior of the non-local quark–quark correlation with LC separation, i.e., the nonlocal quark–quark correlation specified by Equation (23). Because of the limitation of the CQSM, which utilizes a discretized basis for solving the Hartree problem [16,17], this

$E(z_0)$ turns out to be a rapidly fluctuating function of z_0. It is therefore convenient to treat the corresponding smeared function defined as

$$\tilde{E}_\gamma(z_0) \;=\; \frac{1}{\gamma\sqrt{\pi}} \int e^{-(z_0-z)^2/\gamma^2} E(z)\, dz, \tag{25}$$

with a suitable choice of the smearing parameter γ, which we choose here as $\gamma = 0.05$. For the sake of comparison, we also consider the corresponding correlator of the familiar unpolarized PDF,

$$F(z_0) \;=\; \langle N|\, \bar{\psi}\Big(-\frac{z}{2}\Big)\, \gamma^+\, \psi\Big(\frac{z}{2}\Big)\, |N\rangle\, |_{z_3=-z_0, z_\perp=0}, \tag{26}$$

or its smearing version

$$\tilde{F}_\gamma(z_0) \;=\; \frac{1}{\gamma\sqrt{\pi}} \int e^{-(z_0-z)^2/\gamma^2} F(z)\, dz. \tag{27}$$

The upper panel in Figure 9 shows the smeared distribution $\tilde{F}_\gamma(z_0)$ corresponding to the correlator of the unpolarized PDF $f(x)$, while the lower panel represents that corresponding to the smeared distribution $\tilde{E}_\gamma(z_0)$ corresponding to the correlator of the twist-3 PDF $e(x)$. The dashed curves in both figures show the contribution of the three quarks in the valence level, while the solid curves represent the contributions of the quarks in the deformed negative energy Dirac-sea orbits in the mean field. For both distributions, the contributions of the valence quarks denoted by the solid curves are seen to smoothly attenuate as the parameter z_0 as a measure of the light-cone distance becomes larger. In sharp contrast, there is a remarkable difference between the contributions of the Dirac-sea quarks to the correlator $\tilde{F}_\gamma(z_0)$ of the unpolarized PDF $f(x)$ and to the correlator $\tilde{E}_\gamma(z_0)$ of $e(x)$. In spite of the artificial fluctuation behavior arising from the approximate treatment by using the discretized basis, one can clearly see that the Dirac sea contribution to $\tilde{F}_\gamma(z_0)$ approaches zero as z_0 is increased. On the other hand, as seen from the lower panel, the contribution of the Dirac-sea quarks to $\tilde{E}_\gamma(z_0)$ approaches some nonzero constant as z_0 approaches infinity.

To summarize, the preliminary analysis in the CQSM confirms the highly nontrivial behavior of the two types of collation functions as follows,

$$F(z_0) \;\overset{z_0\to\infty}{\longrightarrow}\; 0, \tag{28}$$

$$E(z_0) \;\overset{z_0\to\infty}{\longrightarrow}\; \texttt{nonzero constant}, \tag{29}$$

which makes us convinced that the PDF $e(x)$ has a delta-function singularity at $x = 0$, whereas the PDF $f(x)$ does not.

An interesting question is whether a more realistic lattice QCD simulation gives a similar prediction or not. Unfortunately, the lattice QCD cannot directly handle the light-cone correlators and consequently the standard or usual PDFs. However, instead of usual PDFs, one may consider the *quasi-PDFs*, which are given as Fourier transforms of the space-like correlators. As follows is very brief reminder of the concept of quasi-PDF, which was first introduced in the paper by Ji [44] (see also [45]). Some important properties of the quasi-PDFs are as follows :

- They are defined as Fourier transforms of nucleon matrix element of Lorentz-frame-dependent equal-time correlators in the large nucleon momentum limit.
- They are believed to have the same infrared behaviors as the usual PDFs.
- They are not Lorentz-boost invariant but can be related to the usual PDFs through the matching procedure in the large momentum limit.

- Most importantly, the quasi-PDFs are tractable within the framework of the lattice QCD, since they are related to the space-like correlators instead of the light-cone correlators.

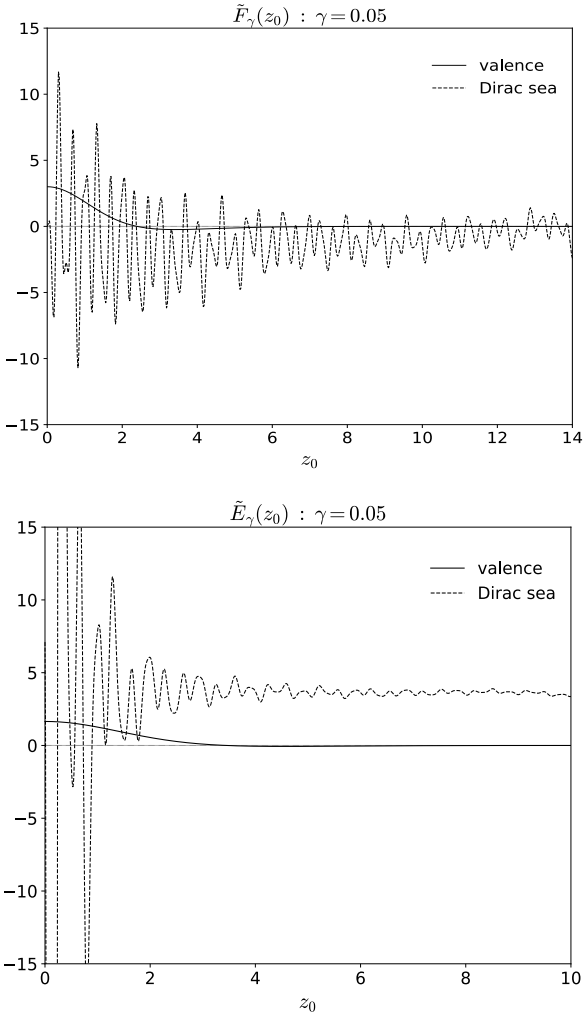

Figure 9. The upper panel here shows the behavior of the smeared distribution $\tilde{F}_\gamma(z_0)$ corresponding to the light-cone correlator of the unpolarized PDF $f(x)$, while the lower panel represents the behavior of the light-cone correlator $\tilde{E}_\gamma(z_0)$ corresponding to the twist-3 PDF $e(x)$.

To be more explicit, we already mentioned that the twist-3 PDF $e(x)$ is obtained as a Fourier transformation of the light-cone correlator $E(z_0)$ as

$$e(x) \;=\; M_N \int_{-\infty}^{\infty} \frac{dz_0}{2\,\pi}\; e^{-i\,x\,M_N\,z_0}\, E(z_0), \tag{30}$$

with

$$E(z_0) \;=\; \langle N \,|\, \bar{\psi}\Big(-\frac{z}{2}\Big)\,\psi\Big(\frac{z}{2}\Big)\,|N\rangle\Big|_{z_3=-z_0,\,z_\perp=0}. \tag{31}$$

The corresponding quasi-PDF $e_{qs}(x)$ is defined as a Fourier transform of the space-like correlator $E_{qs}(z_3)$ as

$$e_{qs}(x) \;=\; M_N \int_{-\infty}^{\infty} \frac{dz_3}{2\,\pi}\; e^{-i\,x\,M_N\,z_3}\, E(z_3), \tag{32}$$

with

$$E_{qs}(z_3) \;=\; \langle N \,|\, \bar{\psi}\Big(-\frac{z_3}{2}\Big)\,\psi\Big(\frac{z_3}{2}\Big)\,|N\rangle\Big|_{z_0=0,\,z_\perp=0}. \tag{33}$$

Since the infrared behaviors of the usual PDF and the quasi-PDF are thought to be the same, we would expect the following behavior for $E_{qs}(z_3)$:

$$E_{qs}(z_3) \quad \stackrel{z_3 \to \infty}{\longrightarrow} \quad \text{nonzero constant.} \tag{34}$$

An interesting challenge is whether the lattice QCD is able to evaluate this correlator and whether it confirms the above conjecture or not.

6. Direct Calculation of $e(x)$ Within the Chiral Quark Soliton Model

Within the framework of the CQSM, we can evaluate the PDF $e(x)$ itself [46]. In fact, it is a little easier to directly evaluate $e(x)$ than to first evaluate the corresponding LC correlator $E(z_0)$. Naturally, the delta-function-type singularity cannot be handled numerically, so it is convenient to first consider the smeared distribution $e_\gamma(x)$ corresponding to $e(x)$:

$$e_\gamma(x) \;\equiv\; \frac{1}{\gamma\sqrt{\pi}} \int_{-\infty}^{+\infty} e^{-(x-x')^2/\gamma^2}\, e(x')\, dx'. \tag{35}$$

Note that a delta-function piece, which we expect is contained in $e(x)$, would appear as a Gaussian function in the smeared distribution $e_\gamma(x)$ with the width γ.

$$e_\gamma(x) \;=\; c\; \frac{1}{\gamma\sqrt{\pi}}\, e^{-x^2/\gamma^2} \quad \Longleftrightarrow \quad e(x) \;=\; c\; \delta(x). \tag{36}$$

A sample result for $e_\gamma(x) \equiv e_\gamma^{(T=0)}(x)$ corresponding to the choice of the parameter $\gamma = 0.06$ is shown in Figure 6. (Here, the superscript $(T=0)$ means the isoscalar combination for quark flavors, i.e., $e^{(T=0)}(x) \equiv e^u(x) + e^d(x)$. We have attached this superscript, since, in the following, we also consider the isovector combination for quark flavors, i.e., the PDF $e^{(T=1)}(x) \equiv e^u(x) - e^d(x)$.) In Figure 10, the solid curve represents the contribution of three quarks in the valence level, whereas the dashed curve represents the contribution of the Dirac-sea quarks. One clearly sees a peak around $x = 0$, the widths of which is the order of γ coming from the Dirac sea contribution, although it deviates from the expected Gaussian shape. (The reason for the deviation from the expected Gaussian form might need some explanation. We said that the vacuum polarization contribution (or the Dirac-sea contribution) to the PDF $e(x)$ is obtained by summing over the contributions of all the negative-energy Dirac-sea orbitals in the hedgehog mean field. This way of evaluating the vacuum polarization contributions is called the calculation based on the "occupied form". Alternatively, the vacuum polarization contribution can be calculated by summing over the contributions of all the positive-energy Dirac-continuum (although actually discretized) orbitals. This way of evaluating the vacuum polarization contributions is called the calculation based on the "unoccupied form". Formally, it was proved that these two ways of calculation should give the same answer, which was in fact verified to be true in the calculations of usual low-energy observables. Unfortunately, there is some difficulty in the calculation of x-dependent PDF $e(x)$. To calculate the vacuum polarization contribution to $e(x)$ in the positive x region, we have used the "occupied form", while to calculate that of $e(x)$ in the negative energy region, we have used the "unoccupied form". The reason is because it is an effective way to obtain $e(x)$ in each region with better numerical precision. Unfortunately, due to the likely existence of the delta-function singularity in $e(x)$ at $x = 0$ as well as the truncation of the discretized Kahana–Ripka basis, this fails to precisely reproduce the expected Gaussian form in the smeared distribution. This is not a serious problem, however, because our demonstration here is to qualitatively convince that the $\delta(x)$-like singularity in $e(x)$ is most likely to exist. (For more, see the following discussion.) Furthermore, we confirmed that as the smearing parameter is made smaller and smaller, the width of the Gaussian-like peak gradually decreases, and the peak eventually disappears when γ becomes smaller than some critical value. This is only natural, since the delta

function cannot be reproduced exactly with the superposition of the truncated discretized basis functions.

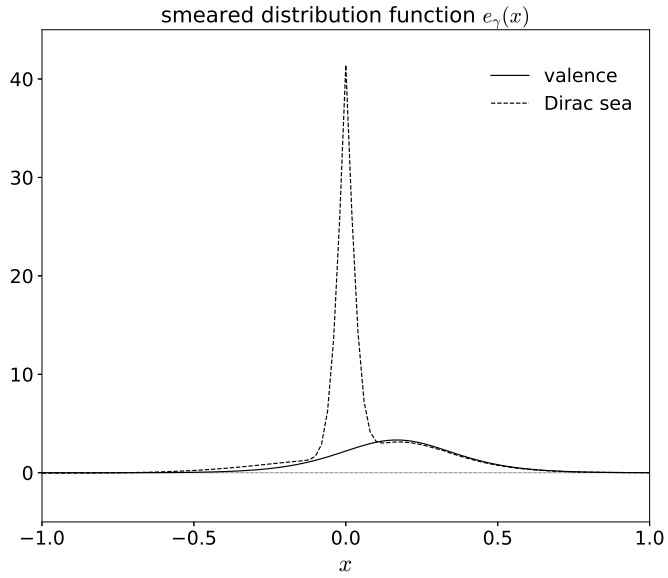

Figure 10. Prediction of the CQSM for the smeared distribution function $e_\gamma(x) \equiv e_\gamma^{(T=0)}(x)$ with a trial choice of the smearing parameter $\gamma = 0.06$.

Because of the extraordinary behavior explained above, the numerical calculation of $e(x)$ needs fairly sophisticated treatment, as explained in [46]. A concise summary of this procedure follows. We start with evaluating the smeared distribution function $e_\gamma(x)$ by using a moderate value of the smearing parameter γ, which reproduces the Gaussian-like peak around $x = 0$. Next, we continue the calculation by gradually decreasing the magnitude of the smearing parameter γ. We then confirm that, as γ is decreased, the width of the Gaussian-like peak gradually decreases, and, at the same time, the fluctuating behavior of the Dirac-sea contribution gradually increases. As the value of γ is further decreased to reach some critical value, we see that the Gaussian-like peak disappears. Since the remaining Dirac-sea contribution shows a fluctuating behavior with the choice of small value of γ, we fit it by an appropriately smooth function, and then we identify it as the regular contribution from the Dirac seas, since its singular contribution corresponding to the delta function at $x = 0$ has already escaped from the numerical simulation.

Figure 11 shows the final numerical prediction of the CQSM for the chiral-odd twist-3 PDF $e^{(T=0)}(x)$ with the isoscalar combination, i.e., $u + d$. The final prediction for $e^{(T=0)}(x)$ is given as a sum of the contribution from the three valence quarks and that from the Dirac-sea quarks as

$$e^{(T=0)}(x) \;=\; e^{(T=0)}_{valence}(x) \;+\; e^{(T=0)}_{sea}(x). \tag{37}$$

The contribution of the Dirac-sea quarks is further divided into the singular contribution, which is proportional to the Dirac delta function $\delta(x)$ as

$$e^{(T=0)}_{sea,singular}(x) \;=\; C\,\delta(x), \tag{38}$$

and the regular contribution as

$$e^{(T=0)}_{sea}(x) \;=\; e^{(T=0)}_{sea,singular}(x) \;+\; e^{(T=0)}_{sea,regular}(x). \tag{39}$$

The regular contribution can be obtained in the numerical procedure as explained above. However, the singular contribution cannot be obtained by the above-explained method, because the delta-function piece escapes from the above numerical procedure. The

question is therefore how to extract the proportionality constant C above the delta-function term. Here, we make use of the fact that the 1st moment of $e^{(T=0)}(x)$ gives the nucleon scalar charge $\bar{\sigma}$. Different from the PDF $e^{(T=0)}(x)$, the scalar charge $\bar{\sigma}$ can be evaluated very precisely within the framework of the CQSM. As a general rule in the CQSM, the nucleon scalar charge is also given as the sum of the valence quark contribution and the Dirac-sea contribution as

$$\bar{\sigma} \;=\; \bar{\sigma}_{valence} \;+\; \bar{\sigma}_{sea} \;\simeq\; 1.7 \;+\; 10.0 \;\simeq\; 11.8. \tag{40}$$

Here, we recall the fact that the Dirac-sea contribution to $\bar{\sigma}$ is related to the 1st moment of the Dirac-sea contribution $e^{(T=0)}_{sea}(x)$ as

$$\bar{\sigma}_{sea} \;=\; \int_{-1}^{1} \Big\{ e^{(T=0)}_{sea,singular}(x) \;+\; e^{(T=0)}_{sea,regular}(x) \Big\}\, dx. \tag{41}$$

Since the regular part of $e^{(T=0)}(x)$, i.e., $e^{(T=0)}_{sea,regular}(x)$ was already obtained by the numerical procedure explained above, its integral can be numerically evaluated without any problem, and the answer is given by

$$\int_{-1}^{1} e^{(T=0)}_{sea,regular}(x)\, dx \;\simeq\; 0.18. \tag{42}$$

Next, after subtracting this regular contribution from the net Dirac-sea contribution to $\bar{\sigma}$, we find that

$$\int_{-1}^{1} e^{(T=0)}_{sea,singular}(x)\, dx \;\simeq\; 9.92, \tag{43}$$

which allows us to determine the proportionality constant C as

$$C \;\simeq\; 9.92. \tag{44}$$

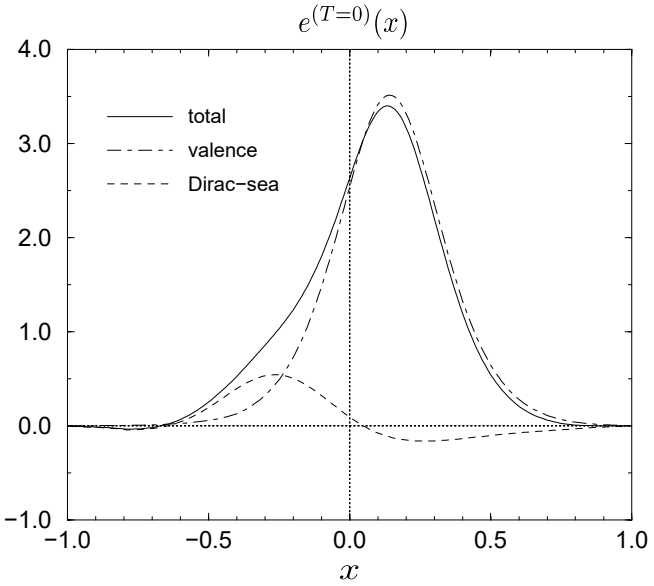

Figure 11. Final prediction of the CQSM for the isoscalar combination of the twist-3 PDF $e(x)$. The dash–dotted and dashed curves here represent the contribution of the three valence quarks and that of the deformed Dirac-sea quarks, while their sum is represented by the solid curves.

Incidentally, with the use of the reasonable value of the average up and down quark mass given by $m_q \simeq (4 \sim 7)\,\mathrm{MeV}$, the prediction of the CQSM for the pion–nucleon sigma term is given by

$$\Sigma_{\pi N} \;=\; m_q\, \bar{\sigma} \;\simeq\; (47 \sim 83)\,\mathrm{MeV}, \tag{45}$$

which seems to favor fairly large values for the pion–nucleon sigma term, which is consistent with the low-energy phenomenology [10–12]. In any case, it is interesting to see that in the CQSM, the dominant contribution to nucleon scalar charge comes from the contribution of the Dirac-sea quarks, especially from the singular delta-function term in the corresponding PDF $e(x)$.

We can also calculate the isovector combination of $e(x)$, i.e., $e^{(T=1)}(x) \equiv e^u(x) - e^d(x)$. Its calculation is much easier than that of the isoscalar piece, because it does not contain a delta-function-like singular piece, which is consistent with that fact that in the QCD vacuum, there is no quark condensate with the isovector combination. We show in Figure 12 the prediction of the CQSM for the isovector combination of the twist-3 PDF $e(x)$. Here, the contribution of the valence quarks and that of the Dirac-sea quarks are, respectively, shown by the dash–dotted and dashed curves, while the total contribution is shown by the solid curves.

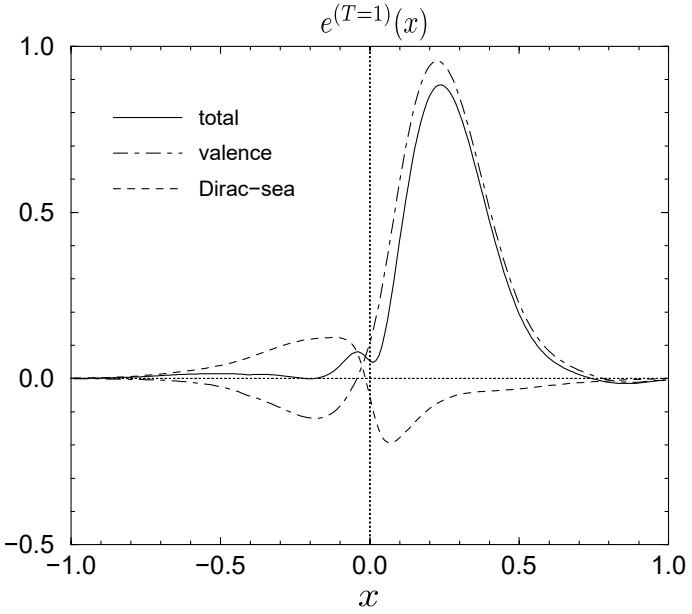

Figure 12. Final prediction of the CQSM for the isovector combination of the twist-3 PDF $e(x)$. The dash–dotted and dashed curves here, respectively, stand for the contribution of the three valence quarks and that of the deformed Dirac-sea quarks, while their sum is represented by the solid curves.

Combining the isoscalar and isovector parts of $e(x)$, we can make a flavor decomposition and obtain any of the following:

$$e^u(x),\ e^d(x),\ e^{\bar{u}}(x),\ e^{\bar{d}}(x) \qquad (x > 0) \tag{46}$$

Here, we have made use of the fact that for the PDF $e(x)$, the calculated distribution function of the quark in the negative x region can be interpreted as the distribution of the corresponding anti-quarks according to the rule $e^q(-x) = e^{\bar{q}}(x)$ with $0 < x < 1$.

Figure 13 shows the preliminary comparison of the prediction of the CQSM for the twist-3 PDF $e(x)$ with the flavor combination $e^u(x) + \frac{1}{4}\, e^{\bar{d}}(x)$ with the empirical extraction of the corresponding PDF at $Q^2 \simeq 5\,\mathrm{GeV}$ from the CLAS semi-inclusive scattering data. Although the comparison is very preliminary, the agreement between the theoretical prediction and the empirical data is encouraging. We emphasize the fact that the theoretical curve here contains only the sum of the three valence quarks contribution and the regular part of the Dirac-sea contribution, and these contributions are far much smaller than the singular part of the Dirac-sea contribution, which is concentrated at $x = 0$ as a Dirac delta function. This observation together with rough agreement between the theory and the empirical data already appear to support the likely existence of the delta-function singularity in $e(x)$ with sizable strength. Naturally, to collect more confirmative evidence,

more precise extraction of the PDF $e(x)$ from the analysis of the relevant semi-inclusive processes is mandatory especially down to the small x region as much as possible. (For a more recent experimental status, see [47,48], for example). If this becomes in fact possible, we may be able to confirm the existence of the delta function in $e(x)$ as a signal of the nontrivial vacuum structure of QCD even though somewhat indirectly.

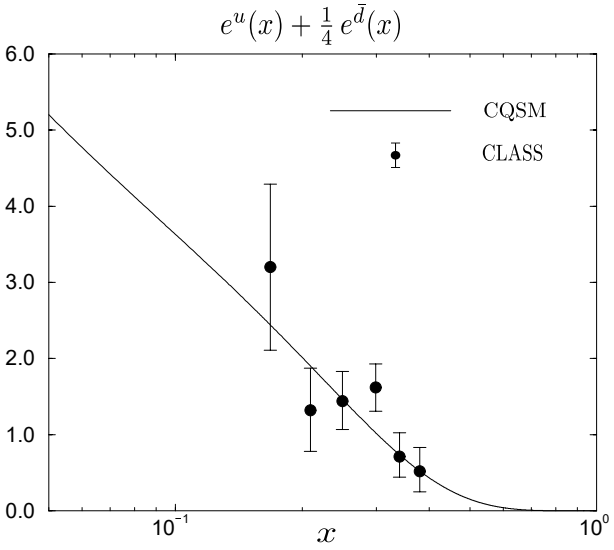

Figure 13. Preliminary comparison of the CQSM for the twist-3 PDF $e(x)$ of the flavor combination $e^u(x) + \frac{1}{4}\, e^{\bar{d}}(x)$ corresponding to the energy scale $Q^2 \simeq 5\,\mathrm{GeV}$ with the empirical data extracted from the CLAS measurement by Efremov, Goeke and Schweitzer [49].

7. Summary

The CQSM predicts fairly unusual behavior of the nucleon scalar charge densities as follows:

- $\langle N \,|\, \bar{\psi}\, \psi \,|\, N \rangle_r \overset{r\to\infty}{\longrightarrow}$ `nonezero constant;`
- existence of $\delta(x)$-type singularity in the chiral-odd twist-3 PDF $e(x)$.

These predictions of the chiral quark soliton model (CQSM) for the chiral-odd twist-3 PDF $e(x)$ come from its unique feature such that it can simultaneously describe the nontrivial vacuum quark condensate and the local structure of the nucleon scalar charge distribution. An interesting question is whether the lattice QCD simulation would confirm these unique predictions of the CQSM in the scalar channel, which has the same quantum number as the physical vacuum. As is well known, although the light-cone PDFs cannot be handled by the lattice QCD framework, the corresponding quasi-PDFs would in principle be tractable. Due to the nontrivial behavior of the QCD vacuum characterized by the nonzero quark condensate, such a simulation in the scalar channel would not be very easy, but it must be a great challenge to the framework of lattice QCD.

From the experimental side, the precise extraction of the PDF $e(x)$ is not an easy task. This is because its chiral-odd nature forbids its measurement through the well-understood inclusive deep-inelastic scatterings (DIS). To extract it, one must use more complicated semi-inclusive DIS processes. Moreover, the delta-function singularity at $x = 0$ cannot be directly accessed through the framework of the high-energy deep-inelastic scattering measurement. The best one can do is to extract $e(x)$ down to the smallest possible value of $x = x_{min}$ and evaluate its integral over x between x_{min} and 1. If the coefficient of the delta-function term is as large as that predicted by the CQSM, this integral would significantly underestimate the value of the nucleon scalar charge as expected from the pion–nucleon sigma term sum rule. It appears to us that several preliminary analyses already indicate the validity of this anticipation.

Funding: This research received no external funding.

Data Availability Statement: Dataset available on request from the authors.

Acknowledgments: The present paper is based on the author's talk at Journal Club at KEK in 2021. The author would like to thank the members of KEK Theory Center for critical but constructive discussions and advice.

Conflicts of Interest: The author declares no conflicts of interest.

References

1. Jameson, I.; Thomas, A.W.; Chanfray, G. The pion-nucleon sigma term. *J. Phys. G Nucl. Part. Phys.* **1992**, *18*, L159–L165. [CrossRef]
2. Sainio, M.E. Pion-nucleon sigma-term—A review. *arXiv* **2001**, arXiv:0110413.
3. Cottingham, W.N.; Greenwood, D.A. *An Introduction to the Standard Model of Particle Physics*, 2nd ed.; Cambridge University Press: New York, NY, USA, 2007.
4. Schwartz, M. *Quantum Field Theory and the Standard Model*; Cambridge University Press: New York, NY, USA, 2014.
5. Courtoy, A.; Baeßler, S.; González-Alonso, M.; Liuti, S. Beyond-Standard-Model Tensor Interaction and Hadron Phenomenology. *Phys. Rev. Lett.* **2015**, *115*, 162001. [CrossRef] [PubMed]
6. Courtoy, A. The Tensor and the Scalar Charges of the Nucleon from Hadron Phenomenology. *EPJ Web Conf.* **2018**, *172*, 03007. [CrossRef]
7. Yamanaka, N.; Hashimoto, S.; Kaneko, T.; Ohki, H. Nucleon charges with dynamical overlap fermion. *Phys. Rev. D* **2018**, *98*, 054516. [CrossRef]
8. Hasan, N.; Green, J.; Meinel, S.; Engelhardt, M.; Krieg, S.; Negele, J.; Pochinski, A.; Syritsyn, S. Nucleon axial, scalar, and tensor charges using lattice QCD at the physical pion mass. *Phys. Rev. D* **2019**, *99*, 114505. [CrossRef]
9. Alexandrou, C.; Bacchio, S.; Constantinou, M.; Finkenrath, J.; Hadjiyiannakou, K.; Jansen, K. Nucleon axial, tensor, and scalar charges and σ-term in lattice QCD. *Phys. Rev. D* **2020**, *102*, 054517. [CrossRef]
10. Gasser, J.H.; Leutwyler, H.; Sainio, M.E. Sigma-term update. *Phys. Lett. B* **1991**, *253*, 252–259. [CrossRef]
11. Hoferichter, M; de Elvira, J.R.; Kubis, B; Meißner, U.-G. High-Precision Determination of the Pion-Nucleon σ Term from Roy-Steiner Equations. *Phys. Rev. Lett.* **2015**, *115*, 092301. [CrossRef]
12. Hoferichter, M.; de Elvira, J.R.; Kubis, B; Meißner, U.-G. On the role of isospin violation in the pion-nucleon σ-term. *Phys. Lett. B* **2023**, *843*, 1–6. [CrossRef]
13. Johnson, K. The M.I.T. bag model. *Acta Phys. Pol.* **1975**, *B6*, 865–892.
14. Brodsky, S.J.; Roberts, C.D.; Shrock, R.; Tandy, P.C. New perspective on the quark condensate. *Phys. Rev. C* **2010**, *82*, 022201(R). [CrossRef]
15. Diakonov, D.I.; Petrov, V.Y.; Pobylitsa, P.V. A chiral theory of nucleons. *Nucl. Phys. B* **1988**, *306*, 809. [CrossRef]
16. Kahana, S.; Ripka, G. Baryon density of quarks coupled to a chiral field. *Nucl Phys. A* **1984**, *429*, 462. [CrossRef]
17. Wakamatsu, M.; Yoshiki, H. A Chiral Quark Model of the Nucleon. *Nucl Phys. A* **1991**, *524*, 561–600. [CrossRef]
18. Kubota, T.; Wakamatsu, M.; Watabe, T. Chiral quark soliton model with Pauli-Villars regularization. *Phys. Rev. D* **1999**, *60*, 014018. [CrossRef]
19. Diakonov, D.; Petrov, V.; Pobylitsa, P.; Polyakov, M.; Weiss, C. Nucleon parton distributions at low normalization point in the large N_c limit. *Nucl. Phys. B* **1996**, *480*, 341–378. [CrossRef]
20. Diakonov, D.; Petrov, V.; Pobylitsa, P.; Polyakov, M.; Weiss, C. Unpolarized and polarized quark distributions in the large N_c limit. *Phys. Rev. D* **1997**, *56*, 4069–4083. [CrossRef]
21. Weigel, H.; Gamberg, L.; Reinhardt, H. Nucleon structure functions from a chiral soliton. *Phys. Lett. B* **1997**, *399*, 287–296. [CrossRef]
22. Weigel, H.; Gamberg, L.; Reinhardt, H. Polarized nucleon structure functions withoin a chiral soliton model. *Phys. Rev. D* **1997**, *55*, 6910–6923. [CrossRef]
23. Wakamatsu, M.; Kubota, T. Chiral symmetry and the nucleon spin structure functions. *Phys. Rev. D* **1999**, *60*, 034020. [CrossRef]
24. Wakamatsu, M. Light-flavor sea-quark distributions in the nucleon in the SU(3) chiral quark soliton model. I. Phenomenological predictions. *Phys. Rev. D* **2003**, *67*, 034005. [CrossRef]
25. Wakamatsu, M. Light-flavor sea-quark distributions in the nucleon in the SU(3) chiral quark soliton model. II. Theoretical formalism. *Phys. Rev. D* **2003**, *67*, 034006. [CrossRef]
26. Wakamatsu, M. On the new COMPASS measurement of the deuteron spin-dependent structure function g_1^d. *Phys. Lett. B* **2007**, *646*, 24–28. [CrossRef]
27. Adeva, B.; Akdogan, T.; Arik, E.; Arvidson, A.; Badelek, B.; Bardin, G.; Baum, G.; Berglund, P.; Betev, L.; Bird, I.G.; et al. Spin asymmetries A_1 and structure functions g_1 of the proton and the deuteron from polarized high energy muon scattering. *Phys. Rev. D* **1998**, *58*, 112001. [CrossRef]
28. COMPASS Collaboration; Ageev, E.S.; Alexakhin, V.Y.; Alexandrov, Y.; Alexeev, G.D.; Amoroso, A.; Badełek, B.; Balestra, F.; Ball, J.; Baum, G.; et al. Measurement of the spin structure of the deuteron in the DIS region. *Phys. Lett. B* **2005**, *612*, 154–164. [CrossRef]

29. COMPASS Collaboration; Alexakhin, V.Y.; Alexandrov, Y.; Alexeev, G.D.; Alexeev, M.; Amoroso, A.; Badełek, B.; Balestra, F.; Ball, J.; Barth, J.; et al. The deuteron spin-dependent structure function g_1^d and its first moment. *Phys. Lett. B* **2007**, *647*, 8–17. [CrossRef]
30. Airapetian, A.; Akopov, N.; Akopov, Z.; Andrus, A.; Aschenauer, E.C.; Augustyniak, W.; Avakian, R.; Avetissian, A.; Avetissian, E.; Belostotski, S.; et al. Precise determination of the spin structure function g_1 of the proton, deuteron, and neutron. *Phys. Rev. D* **2007**, *75*, 012007. [CrossRef]
31. de Florian, D.; Sassot, R.; Strattmann, M.; Vogelsang, W. Extraction of spin-dependent parton densities and their uncertaintities. *Phys. Rev. D* **2009**, *80*, 034030. [CrossRef]
32. Ackerstaff, K.; Airapetian, A.; Akopov, N.; Akushevich, I.; Amarian, M.; Ashenauer, E.C.; Avakian, H.; Avakian, R.; Avetissian, A.; Bains, B.; et al. Flavor Asymmetry of the Light Quark Sea from Semi-inclusive Deep-Inelastic Scattering. *Phys. Rev. Lett.* **1998**, *81*, 5519–5523. [CrossRef]
33. Towell, R.S.; McGaughey, P.L.; Awes, T.C.; Beddo, M.E.; Brooks, M.L.; Brown, C.N.; Bush, J.D.; Carey, T.A.; Chang, T.H.; Cooper, W.E.; et al. Improved measurement of the $\bar{u}/\bar{u}$ asymmetry in the nucleon sea. *Phys. Rev. D* **2001**, *64*, 052002. [CrossRef]
34. NA51 Collaboration; Baldit, A.; Barriere, C.; Castor, J.; Chambon, T.; Devaux, A.; Espagnon, B.; Fargeix, J.; Force, P.; Landaud, G.; et al. Study of the isospin symmetry breaking in the light quark sea of the nucleon from the Drell-Yan process. *Phys. Lett. B* **1994**, *332*, 244–250. [CrossRef]
35. Reinhardt, H.; Weigel, H. Vacuum nature of the QCD condensates. *Phys. Rev. D* **2012**, *85*, 074029. [CrossRef]
36. Kodaira, J.; Tanaka, K. Polarized Structure Functions in QCD. *Prog. Theor. Phys.* **1999**, *101*, 191–242. [CrossRef]
37. Burkardt, M.; Koike, Y. Violation of sum rules for twist-3 parton distributions in QCD. *Nucl. Phys. B* **2002**, *632*, 311–329. [CrossRef]
38. Efremov, A.V.; Schweitzer, P. The chirally-odd twist-3 distribution $e^a(x)$. *J. High Energy Phys.* **2003**, *08*, 006. [CrossRef]
39. Schweitzer, P. The chirally-odd twist-3 distribution function $e(x)$ in the chiral quark-soliton model. *Phys. Rev. D* **2003**, *67*, 114010. [CrossRef]
40. Wakamatsu, M.; Ohnishi, Y. Nonperturbative origin of the delta-function singularity in the chirally odd twist-3 distributio function $e(x)$. *Phys. Rev. D* **2003**, *67*, 114011. [CrossRef]
41. Ma, J.P.; Zhang, G.P. On the singular behavior of the chirally-odd twist-3 parton distribution $e(x)$. *Phys. Lett. B* **2020**, *811*, 135947. [CrossRef]
42. Bhattacharya, S.; Cichy, K.; Constantinou, M.; Metz, A.; Scapellato, A.; Stefenns, F. The role of zero-mode contributions in the matching for the twist-3 PDFs $e(x)$ and $h_L(x)$. *Phys. Rev. D* **2020**, *102*, 114025. [CrossRef]
43. Hatta, Y.; Zhao, Y. Parton distribution function for the gluon condensate. *Phys. Rev. D* **2020**, *102*, 034004. [CrossRef]
44. Ji, X. Parton Physics on a Euclidean Lattice. *Phys. Rev. Lett.* **2013**, *110*, 262002. [CrossRef] [PubMed]
45. Ji, X.; Zhang, J.-H.; Zhao, Y. Physics of the Gluon-Helicity Contribution to Proton Spin. *Phys. Rev. Lett.* **2013**, *111*, 112002. [CrossRef] [PubMed]
46. Ohnishi, Y.; Wakamatsu, M. πN sigma term and chiral-odd twist-3 distribution function $e(x)$ of the nucleon in the chiral quark soliton model. *Phys. Rev. D* **2004**, *69*, 114002. [CrossRef]
47. Courtoy, A. Insight into the higher-twist distribution $e(x)$ at CLASS. *arXiv* **2022**, arXiv:1405.7659.
48. Courtoy, A.; Miramontes, A.; Avakian, A.H.; Mirazita, M.; Pisano, S. Extraction of the higher-twist parton distribution $e(x)$ from CLAS data. *Phys. Rev. D* **2022**, *106*, 014027. [CrossRef]
49. Efremov, A.V.; Goeke, K.; Schweitzer, P. Azimuthal asymmetries in SIDIS and Collins analysing power. *Nucl. Phys. A* **2002**, *711*, 84–88. [CrossRef]